NASA-CR-202811

BUOYANT DOWNWARD DIFFUSION FLAME SPREAD AND EXTINCTION IN PARTIAL-GRAVITY ACCELERATIONS

Kurt R. Sacksteder
NASA Lewis Research Center
Cleveland, Ohio, USA

James S. T'ien
Case Western Reserve University
Cleveland, Ohio, USA

Abstract

This paper describes experimental observations of downward, opposed-flow flame spreading made under partial-gravity conditions aboard NASA research aircraft. Special apparatus and techniques for these tests are described including schlieren imaging of dim near-limit flames. Flame spreading and flammability limit behavior of a thin cellulosic fuel, 1 x 10^{-3} gm/cm^2, tested at 1 atmosphere of pressure in oxygen/nitrogen mixtures of 13%-21% oxygen by volume, is described for effective acceleration levels ranging from 0.05 to 0.6 times normal Earth gravity (1g). Downward burning flammability increases in partial gravity, with the limiting oxygen fraction falling from 15.6% oxygen in 1g to 13%-14% oxygen in 0.05g-0.1g. Flame spread rates are shown to peak in partial gravity, increasing by 20% over the 1g value in air (21% oxygen). Partial-gravity flame spreading results, corrected for fuel density and thickness, are consistent with results obtained at acceleration levels above 1g in a centrifuge. The results compare qualitatively with predictions of flame spreading in buoyant flow by models that include finite rate chemical kinetics and surface and gas-phase radiative loss mechanisms. A correlation of experimental buoyant downward flame-spread results is introduced that accounts for radiative heat losses using a dimensionless spread rate, V_f^*, a radiation/conduction number, S_R, and the Damkohler number, *Da* as parameters. The correlation includes data from 0.05g to 4.25g and oxygen/nitrogen mixtures from 14% oxygen to 50% oxygen.

Introduction

Flame spreading over solid fuels is a phenomena of fundamental interest and of practical value in the study and control of fire. In flame spread studies, distinctions between flames in flows opposed to and concurrent with the flame spread direction, between thermally thin and thick fuels, and between flows imposed externally (forced) or by gravity (buoyancy) have been identified. Several reviews articulate the subject[1,2].

Access to microgravity environments motivated theoretical and experimental explorations of low-speed flow regimes in which buoyancy forces could be reduced or eliminated. Numerical modeling quantified surface and gas-phase radiation mechanisms[3,4,5,6] and predicted the influence of radiative

loss in spread-rate reductions and quenching. Numerical evaluations of velocity-profile effects[7] and predictions that near-wall velocity gradients would correlate spreading behavior[8] led us to suggest separate experimental observations of flames spreading in low-speed purely-forced and purely-buoyant flows.

Purely-forced, opposed flow and quiescent studies in microgravity, using drop-tower[9,10] and Space Shuttle facilities[11], demonstrated the predicted spread rate and quenching effects. In purely buoyant flow, however, downward burning experiments were limited to normal Earth gravity(1g) and elevated gravity using a centrifuge[12]. While noting a low-gravity, quiescent study perturbed by unsteady accelerations[13], this paper reports the first systematic observations of flames spreading in purely-buoyant, low-speed flows induced by accelerations below 1g.

We conducted a series of aircraft-based tests to observe both downward and upward flame-spreading and flammability behavior of thin solid fuels in sustained partial-gravity accelerations between 0.05g and 1g. To obtain these data, special apparatus and techniques were developed. This paper concerns the downward spreading case only, and provides an opportunity to evaluate models of flame spreading in purely buoyant flow.

Experiments

An apparatus was devised to observe flame spread over solid fuels in partial-gravity accelerations aboard NASA aircraft facilities. The apparatus provides semi-autonomous operation, capable of several tests per flight, either attached to the airframe or floated freely in the aircraft cabin. The apparatus includes a 26 liter cylindrical chamber, 25.4 cm in diameter and 50.8 cm in length, simultaneous schlieren and conventional imaging, provisions for atmosphere replacement, thermocouple, ignition and lighting circuitry and a flanged end plate with a quick-release binding for rapid specimen replacement.

Test specimens, 8cm long and 7cm wide, were made of thin cellulosic tissues, tradename Kimwipes, used previously in drop-tower tests[9,10,14]. This material has a half-thickness area density (ie. mass density times thickness) of 1.0mg/cm^2, and was used because of its high flame-spread rate compared to other fuels and because it tends to remain flat while burning. The samples were taped across a 25.4cm x 5cm gap in 0.05cm thick stainless-steel sample holders that fill a diametrical plane of the

cylindrical chamber, thereby exposing fuel, 8cm in the (axial) burning direction by 5cm wide, to the atmosphere on both sides.

Control of the fuel moisture content was constrained. Prior to takeoff, premounted samples were stored in vacuum for approximately 1hr. At altitude, where atmospheric moisture content is low, the samples were exposed to the aircraft-cabin. A vacuum exposure in the test chamber before filling and ignition lasted approximately one minute. Samples were ignited by resistance heating a thin wire for 0.10sec, releasing ≈36j to ignite a strip of nitrocellulose (10.5mg,+/-1%), releasing an additional ≈26j[15] in a flame ball bathing the ignition region. This technique provided a consistent deposition of ignition energy compared to the hot wire used alone.

The test atmosphere was replaced for each test. After replacing the spent test specimen the chamber was evacuated to a pressure of less than 0.008 atmospheres then filled with a commercial oxygen/nitrogen mixture certified to +/-0.03% absolute oxygen content. The residual air after evacuation introduced <0.06% error absolute oxygen content. All experiments were conducted at an initial pressure of 1atm., measured with a transducer calibrated daily.

Flames were visualized with a color schlieren system[16]. The schlieren system was sensitive to the component of the refractive-index gradient normal to the fuel surface, in a cylindrical detection volume 7.9cm in diameter. Ray deflections, attributed to flame-induced density variations, were discriminated at the image plane of the schlieren mirror using a color transparency varying linearly in hue with lateral displacement, then imaged with a video camera. Conventional images of the top view of the flames were recorded using a 16mm motion picture camera operating at 24 frames/second.

The tests were conducted aboard the NASA KC-135 at the NASA Johnson Space Center flying Keplerian trajectories (parabolas) to simulate gravitational accelerations between 0.05g and 0.6g including Lunar (0.16g) and Martian (0.38g) levels[17]. The first parabolas ever attempted at 0.05g and 0.6g were performed for these tests. Local three-axis accelerations were measured with a duplicate of the NASA Space Accelerometer Measurement System[18].

Results

Acceleration Environment

Wind, atmospheric turbulence, and pilot and aircraft performance introduced continuous variation into the measured acceleration levels. Parabolas at the lowest set points (0.05g-0.10g) were perturbed typically by high frequency (>1Hz) variations, often called g-jitter, of about 0.02g. Higher set points (0.16g-0.6g) were additionally perturbed by lower frequency variations (~0.2Hz-1.0Hz) of about 0.04g. The average duration of the parabolas increased with partial-gravity level, from about 8 seconds for the shortest 0.05g parabola to about 50 seconds for most 0.6g parabolas. The parabolas begin and end with a pull-up maneuver at just under 2.0g, to which some flames were exposed.

Flammability

Figure 1 summarizes the test matrix and shows a flammability boundary based on acceleration level and atmospheric oxygen content. In 1g the same apparatus and fuel (5 cm wide) were used to determine the limit using partial-pressure mixtures of the certified 15% and 16% mixtures. In 1g, the specimens never burned more than 2-3cm below the ignitor in 15.5%O_2, usually burned 4-5cm, but never the full 8cm, in 15.6%O_2, and usually, but not always, burned the full 8cm in 15.7%O_2. Completely burning 0.08gm of cellulose reduces (by calculation) the oxygen in the chamber from 15.6% to 15.53%, constraining the limit determination to a precision of about 0.1%. Based on the behavior described, a 1g limit of 15.6%O_2 is shown in Fig 1.

Obtaining the precision of the 1g limit criteria was not practical in the aircraft because test opportunities are limited. In 14%O_2 at 0.18g and 0.38g, flames propagated 1.4cm and 0.4cm, respectively, and quenched before the onset of high accelerations, while in 15%O_2 (same accelerations) the samples burned completely. In 14%O_2 at 0.05g and 0.1g, flames progressed 3.1cm and 2.4cm, respectively, spreading in partial gravity for 8-9 seconds then extinguishing during high accelerations. These are interpreted as flammable conditions. Samples ignited in 13%O_2 quickly quenched.

The reported 1g downward-burning limit of 16.0% - 16.5%O_2 for 3cm wide samples of this fuel,[9] was slightly higher than results obtained with 3cm wide samples in the aircraft apparatus, where using the above propagation criteria provided a limit of 15.8%O_2. The earlier tests were ignited with a

heated wire and may have been influenced by a nearby mirror present to obtain an orthogonal view. The higher flammability limit might be attributed to differences in the useful ignition energy or heat losses to the mirror. This comparison suggests that the quiescent microgravity limit of 21%O_2 (the logical extreme of the buoyant-flow case), obtained in drop tower tests[9], is reasonable to within 1%O_2. However, because drop-tower accelerations have not been measured, that limit could not be included in Fig. 1. Limiting accelerations between 4.0g and 4.25g in 21%O_2 for a similar fuel were reported in centrifuge tests,[12] and are shown in Fig. 1.

Reducing accelerations from 4g to 0.05g monotonically enhances downward burning flammability. The microgravity limit of 21%O_2 implies, however, that the flammability boundary curves upward at smaller accelerations and that a minimally-flammable oxygen environment exists for this fuel, for downward burning, at or below 0.05g. The analogous flammability boundary, predicted by a numerical model[6], is included in Fig. 1 for comparison and later discussion.

Flame Imaging

Recorded schlieren flame images were fundamentally different from earlier gravity-related flame spreading results. Visible-light emissions from near-limit flames in microgravity tests are dim and difficult to capture by direct imaging, either video or motion picture film[9,10,11,13,14]. Measures to enhance film images, including forced film processing, low framing rates, and small f/numbers, reduce flame tracking precision. Short focal-length lenses, typical of compact microgravity experiment designs, introduce spatial distortions from magnification variations across wide flames.

Schlieren imaging provided increased dim-flame detection sensitivity and constant image magnification across the flame width. At ignition, an expanding ball of heated gases was visible to the schlieren system, reaching 2-3cm below (upstream of) the ignitor (for <1sec) before buoyancy displaced it upward. Conventional visible photography showed a smaller flame surrounding the ignitor. Extinguishing flames were clearly defined in the schlieren images, shrinking to ≤2-3mm in length before disappearing. Figure 2 shows schlieren images of a flame spreading first at 0.1g in 15%O_2, a non-flammable condition in 1g, then as the flame nears blowoff extinction at higher accelerations at the end of the test.

Flame Spread

Flame propagation rates were obtained from the schlieren results. Figure 3 shows the flame displacement with time, synchronized with the component parallel to the flame spreading direction of the instantaneous local acceleration, for a test in 15%O_2, where the slope of the displacement plot indicates flame spread rate. At the end of the parabola, the increase in local acceleration accompanied a slowed, then extinguished, flame. Figure 2 shows schlieren images from that test before and during the higher accelerations, illustrating how the flame narrowed as it approached extinction. The flame was extinguished as the local accelerations crossed the flammability boundary of Fig. 1, at about 0.6g.

Spread-rates were influenced by g-jitter to the extent that reporting spread rates averaged over the test time showed unacceptable scatter. The partial-gravity results, shown in Fig. 4, were obtained, instead, by measuring flame displacements during brief time periods, ≥3 seconds, of smaller g-jitter. This procedure was considered acceptable since flames responded to perturbations in much less than one second (eg. at time ≈10sec. in Fig. 3). Figure 4 also includes 1g results, obtained in the aircraft, drop-tower[9], and centrifuge[12] test chambers, and centrifuge data in 21%O_2 up to 4.25g. All spread rates are corrected for fuel area density, ρ_{area}, where $\rho_{area} = \rho_{mass} \cdot \tau$, the mass density times the fuel half-thickness. This correction follows from the assertion in the early heat transfer model[19] that $\rho_{area} \cdot V_f$=constant for thin fuels and has been used successfully[9,10,12].

Partial-gravity spread rates in 21%O_2 fall naturally along the trend of the centrifuge data, peak at an acceleration level near 0.6g, then decline with further decreases in acceleration. Spread rates at 1g from the three different test chambers agree to within 5%. Prediction of spread rate behavior for a thin fuel in 21%O_2 from a numerical model[6], corrected for ρ_{area}, is included for comparison and later discussion. Spread rates in 18%O_2 show a similar non-monotonic spread-rate variation with acceleration. Spread rates in 14%O_2 to 16%O_2 show only the downward slope.

Discussion

Comparison with Theory

Two numerical models predict downward flame spreading behavior at partial-gravity accelerations[6,8]. Both calculations utilize a one-step, finite-rate, gas-phase chemical reaction model and estimate radiative losses from both the fuel surface and the gas-phase. Reference 8 presents calculated spread rates and extinction limits in 50%O_2-50%N_2, 1.5atm, from 10^{-6}g to 10g; and in

$21\%O_2$-$79\%N_2$ at 1g-4g. Reference 6 presents spread rates and extinction limits in $21\%O_2$-$79\%N_2$, at 1atm from 0.012g-4.3g, and a flammability boundary over the same range of accelerations. The data of reference 6 are included as the dotted lines in Figs. 1 and 4.

The predictions of spread rate show qualitatively the peak spread rate feature observed experimentally in $21\%O_2$ and $18\%O_2$ at intermediate gravity levels. From the peak, falling spread rates at higher gravity are attributed to decreased reactant residence time in the flame zone (compared to the chemical reaction time) and reduced forward heat transfer from flames receding with respect to the pyrolysis front. Falling spread rates at lower gravity are attributed to lower flame temperatures, resulting from an increasing ratio of radiative loss to chemical heat release, and reduced forward heat transfer from cooler flames farther from the fuel surface. The spread rate predictions of reference 6 for $21\%O_2$ are higher (Fig. 4) than experimentally observed in partial gravity, though they agree well with experiments at normal gravity and above. The predictions in reference 8 also reproduce observed experimental results at and above 1g, in $21\%O_2$ as shown and also in $50\%O_2$, 1.5atm.

Both models predict a high-gravity extinction limit (viz. a blowoff limit) and a low-gravity extinction limit (viz. a radiative quenching limit). These flammability limits are attributed to the dominance of the flame-retarding mechanisms described above. The flammability boundary predicted in reference 6 (Fig. 1) is U-shaped, showing a minimally-flammable oxygen concentration between 0.2-0.3g. The flammability boundary suggested by the experimental data does not show such a minimum, but the reported quiescent microgravity limit for this fuel, $21\%O_2$[9], suggests it exists $\leq$0.05g. The predicted flammability boundary agrees well with experimental observations above normal gravity, but diverges from the observed boundary at normal gravity ($13.3\%O_2$ vs $15.6\%O_2$) and below ($21\%O_2$ limit at 0.012g vs $\approx$microgravity[9]).

The sources of discrepancy between prediction[6] and observed partial-gravity flammability and spread-rate behavior are not clear, but may involve the choice of kinetic and radiation parameters. The spread-rate peak and the (presumed) minimum-oxygen limit arise from competition, under finite kinetics, between the heat-release rate reduction (due to shortened residence time), and the radiative heat-loss rate. An underestimation of the radiative loss rate compared to the chemical reaction rate might explain the differences at 1g and the partial-gravity levels, but would not reconcile the limiting accelerations in 21% oxygen.

Flame Spread Rate Correlation

Correlations of measured flame spread rates have been achieved for purely buoyant flows[12] and for forced-convection flows in normal gravity[20] using formulations of dimensionless spread rate, V_f^*, versus Damkohler number, *Da*. Formulations of *Da*, nominally a ratio of reactant residence time in the flame to chemical reaction time, have included simple pre-exponential chemical models (without Arrhenius factors)[21,6], models with strong flame temperature dependence[12], and additional provisions for fuel-vapor diffusion from the surface[20]. Velocity characterizations for residence-time estimates have included a buoyant velocity, $V_b=(\alpha g(T_f-T_\infty)/T_\infty)^{1/3}$[21,12,8], where T_f and T_∞ are flame and ambient temperatures and α is the thermal diffusivity; or the freestream velocity, U_∞, alone[20] or including consideration of the boundary layer structure[22]. V_f^*, corrected for ρ_{area}, is a ratio of actual spread rate to the spread rate possible without heat loss in the infinite chemical-rate limit[19]. Where the flame-retarding mechanism is associated with limited residence time, *Da* correlations of flame-spread rates are successful. This approach does not succeed with data from microgravity forced flows, nor with the partial-gravity data, because it does not account for radiative losses from these flames.

We revisited the formulation of the data correlation for purely-buoyant flame spread data[12], to include the partial-gravity data. We evaluated *Da* similarly:

$$Da = \frac{B\lambda m_{ox,\infty}}{c_p M_{ox} V_b^2} \cdot \left(\frac{RT_f}{E} \cdot \frac{T_f}{\left(\frac{\Delta H_c m_{ox,\infty}}{i\, c_p} \right)} \right)^3 \cdot \exp\left(-\frac{E}{R T_f} \right)$$

where the pre-exponential constant $B=5.69 \cdot 10^9$ m^3/mole-sec, the activation energy, E=167.35 Kj/Kg-K, the heat of combustion, ΔH_c=16,740 Kj/Kg, $m_{ox,\infty}$ and M_{ox} are the ambient O_2 mass fraction and molecular weight, the stoichiometric oxygen/fuel mass ratio, i=1.185, and λ and c_p are the gas thermal conductivity and specific heat, evaluated for the initial O_2/N_2 mixtures at the fuel vaporization temperature, T_v=618K. We evaluated T_f differently, however, using the STANJAN equilibrium code for a stoichiometric, adiabatic flame temperature, allowing for dissociation, and evaluated V_b using T_f. The pre-exponential constant, which does not affect the shape of the resulting data presentation, was adjusted from the literature value[12] to bring *Da*=1 at blowoff extinction. The grouping

$(\Delta H_c m_{ox,\infty}/i c_p)$ in the cubic factor is a reference temperature[12] that varies only with the explicit O_2 content.

The dimensionless spread rate, defined[12] as

$$V_f^* = \frac{V_f}{V_{f,\infty}} = \rho_{area} V_f \cdot \frac{c_s (T_v - T_\infty)}{\sqrt{2}\lambda (T_f - T_v)}$$

where $V_{f,\infty}$ is the spread rate in the no-loss, infinite-kinetics limit, and the solid-fuel specific heat, c_s=1.26Kj/Kg-K. A radiation parameter, S_R, derived through dimensional analysis of the energy equation[3,4,6] as a ratio of radiation to conduction over one thermal length, $S_R = (\sigma T_\infty^4)/(\lambda T_\infty/(\alpha/V_r)) = \sigma T_\infty^3/\rho c_p V_r$ where σ is the Stefan-Boltzmann constant, and V_r is the reference velocity for the flow (in the buoyant case, $V_r = V_b$). We have used S_R as a correction to V_f^*, suggesting that it estimates the additional spread-rate deficit, due to radiative heat loss, from the no-loss maximum spread rate. Figure 5 shows a plot of $V_f^* \cdot S_R$ vs *Da* for flames spreading in purely-buoyant flow, in partial-gravity (data of Fig. 4) and in the centrifuge (21%O_2 and 50%O_2, 1atm from 1g-4g[12]).

We considered that calculating T_f independently while using c_p and ΔH_c evaluated as in reference 12 might suggest an inconsistency in evaluating $V_f^* \cdot S_R$ and *Da*. T_f values estimated using ΔH_c, c_p evaluated at T_v for the O_2/N_2 mixture, and without dissociation[12], are much higher than ours, which we believe to be more realistic. A correct c_p value is implicit, however, in the equilibrium calculation, allowing dissociation, of T_f. Remaining uncertainty in calculating T_f lies in the chosen value of ΔH_c, which both formulations use. The roles of c_p and λ in $V_f^* \cdot S_R$ and *Da* are primarily associated with forward heat conduction, so the evaluation for the ambient O_2/N_2 mixture at an intermediate temperature, T_v, is appropriate. The constant ΔH_c, i, and c_p in the reference temperature do not affect the shape of the data presentation.

This presentation smooths the scatter in spread rates seen in Fig. 4. The scatter has no trend attributable to O_2 content. The data in 21%O_2 span the acceleration range of 0.05g to 4.25g and also the length of the correlation curve, while the data in 50%O_2 span only 1g-4g and lie within the 21%O_2 data. Near blowoff extinction, $V_f^* \cdot S_R$ vs *Da* values for 15%O_2,≈0.6g, 16%O_2,≈1g, and 21%O_2,4.25g lie together at the left-hand end of the curve.

Conclusions

Using parabolic trajectories in aircraft, we have conducted the first experiments in buoyant diffusion-flame spread over a thin solid in a partial-gravity range of 0.05 to 0.6 times normal Earth gravity. To operate successfully in this unusual environment required the development of special apparatus and techniques including: a schlieren system for imaging dim near-limit flames, a fast acting and repeatable ignition system, precise acceleration measurements, and extending the range of accelerations provided by the aircraft flight crew.

Using gravity as a variable parameter provided a new means to study the effect of convection on flame spread and extinction processes. Unlike experiments in forced flow where the local velocity in front of the flame depends both on the free-stream velocity and the developing boundary layer, the local velocity in front of the flame in buoyant flow depends only on the gravity level.

Downward spreading flames were observed in partial gravity in O_2/N_2 mixtures between 14%O_2 and 21%O_2 at normal atmospheric pressure, demonstrating peak values of flame spread rate and increased flammability at local accelerations below normal Earth gravity. Flame spread rates 20% higher than in normal gravity were observed in partial gravity, and flammability increased, with the limiting oxygen fraction falling from 15.6%O_2 in normal gravity to 13%-14%O_2 at 0.05-0.1g.

A data presentation with a radiative correction to dimensionless downward flame spread rates correlates with Damkohler numbers in purely-buoyant flows from 0.05g to 4.25g. Comparisons with our data support the qualitative results of theoretical models that include finite-rate chemical kinetics and radiative transport to describe the flame spread and extinction processes. The experimental data provide the basis for improving quantitative predictions from the models.

Acknowledgements

JST would like to gratefully acknowledge the support for his work under NASA grant NAG3-1046. KRS would like to acknowledge the contributions of many associates at the NASA Lewis Research Center, most notably R. Sotos, K. Stambaugh, D. Gotti, D. Griffin, P. Greenberg, and P. Ferkul; and helpful discussions with R. Altenkirch. Finally, both authors would like to acknowledge the support for the work by the Microgravity Science and Applications Division of NASA Headquarters.

(20) Fernandez-Pello, A. C., Ray, S. R., and Glassman, I., Eighteenth Symposium (International) on Combustion, The Combustion Institute, Pittsburgh, 1981, pp.579-589.

(21) Frey, A., and T'ien, J. S., Combust. Flame 36:33 (1976).

(22) Altenkirch, R. A., and Vedha-Nayagam, M., Twenty-Second Symposium (International) on Combustion, The Combustion Institute, Pittsburgh, 1988, pp.1495-1500.

FIG. 1

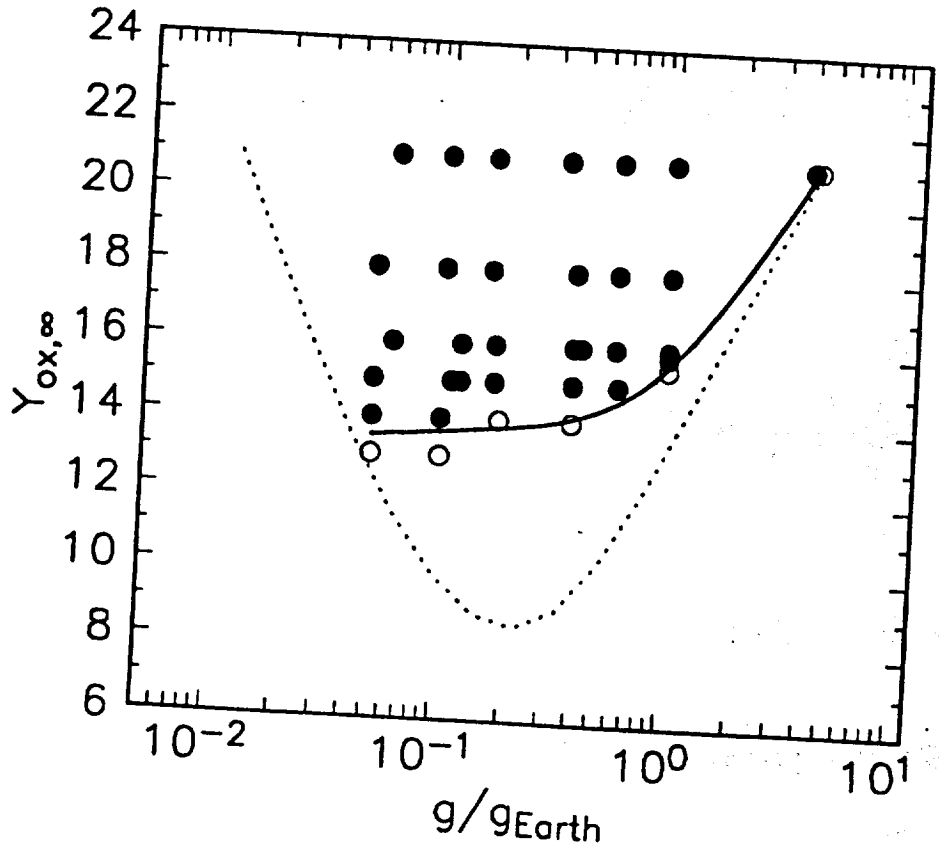

FIG. 3

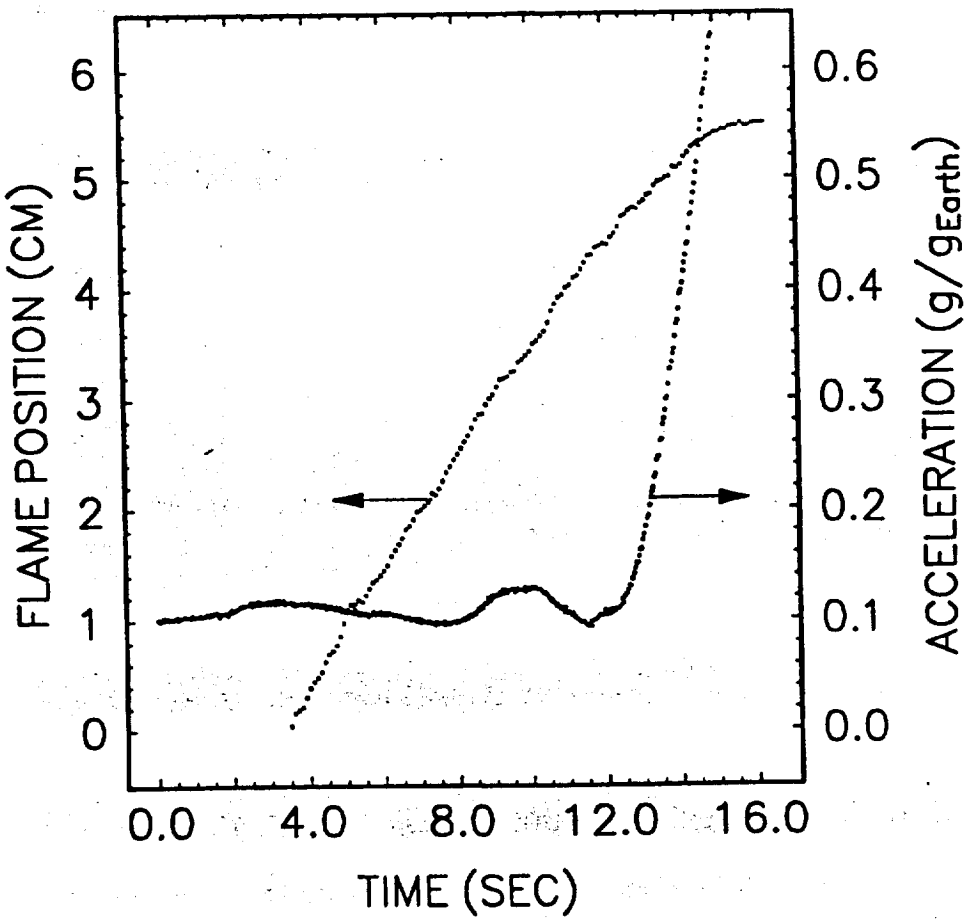
FLAME POSITION (CM)
0
1
2
3
4
5
6
ACCELERATION (g/gEarth)
0.0
0.1
0.2
0.3
0.4
0.5
0.6
0.0
4.0
8.0
12.0
16.0
TIME (SEC)

FIG. 5

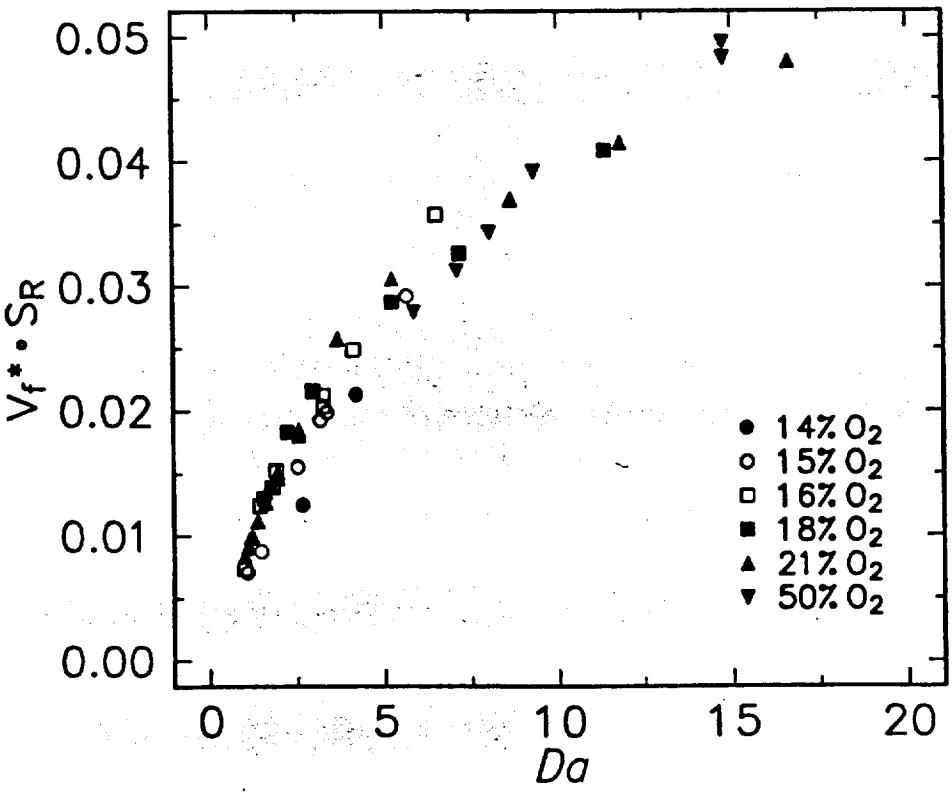
0.05
0.04
0.03
0.02
0.01
0.00
$V_f^* \cdot S_R$
0
5
10
15
20
Da
14% O_2
15% O_2
16% O_2
18% O_2
21% O_2
50% O_2